Effects of Precursor Salt on Colloidal Cobalt Oxyhydroxides Composition and Its Application in Non-Enzymatic Glucose Electrooxidation

Andreia Stadnik, Filipe Q. Mariani and Fauze J. Anaissi*

Departamento de Química, Universidade Estadual do Centro-Oeste, 85040-080, Guarapuava - PR, Brazil.

Received 14 March 2017, revised 15 August 2017, accepted 17 August 2017.

ABSTRACT

Colloidal cobalt oxyhydroxide [CoO(OH)] has been prepared from precursors cobalt acetate and cobalt nitrate. The cobalt colloids (Co.Acetate and Co.Nitrate) were characterized by simultaneous thermogravimetric/differential thermal analysis, scanning electron microscopy with energy-dispersive X-ray spectroscopy, Fourier transform infrared and electronic spectroscopy. Characterization data indicated the presence of counter ions (CH_3COO^- and NO_3^-), likely intercalated within the structure of the colloidal cobalt. The platinum working electrode chemically modified with cobalt colloid was studied by cyclic voltammetry in alkaline solution [0.5 M, NaOH], which revealed differences in the reproducibility and stability of the electroactive material. The colloidal Co.Nitrate modified electrode was applied to the non-enzymatic glucose (Glu) electrooxidation in the concentration range from 7.2 to 21.9 × 10^{-8} mol L^{-1}. The limits of detection (5.87 × 10^{-8} mol L^{-1}) and quantitation (1.96 × 10^{-7} mol L^{-1}) calculated suggest that colloidal Co.Nitrate has the potential to be used as a sensor for low glucose concentration.

KEYWORDS

Salt inorganic, colloidal cobalt, electrooxidation, low glucose concentration.

1. Introduction

The use of materials with different properties and characteristics always has attracted attention in the field of applied science. Thus, knowing and understanding the physical and chemical properties of the synthesized materials become important parameters in choosing an ideal application. Oxides of transition metals, in particular, cobalt oxides and oxyhydroxides, stand out among the known electroactive materials, which exhibit reversible oxidation states.[1–3]

Among the five species (CoO_2, Co_2O_3, CoO(OH), Co_3O_4 and CoO) known in the literature,[1] cobalt oxyhydroxide [CoO(OH)] has received increased attention due to its semiconducting properties,[4] excellent electrocatalytic activity and chemical stability under alkaline conditions.[2,5] Also, CoO(OH) exhibits reversible electrochemical behaviour,[3] thermal stability and has a high superficial area,[6] leading to increased charge storage rates, and the ability to control its morphology at the micrometric/nanometric scale.[7] The preparation of CoO(OH) can be carried out by a range of methods, such as spraying,[5,8] sol-gel processes,[2,8] hydrothermal techniques,[9] and electrodeposition methods.[5,8] A variety of different precursors and complexing ligands are required for these methods.[2] Both the morphology and composition of the final product depend on factors such as solution precursors, temperature, applied potential, deposition time, and electrode surface.[2]

The use of CoO(OH) has been highlighted due to its application as a magnetic material,[1,6] catalyst,[9,10] a positive electrode in alkaline batteries,[11–16] supercapacitors,[8,17] and CO detection.[13,18] It also promotes the electrooxidation of various organic molecules,[5] thereby constituting a sensor for analytes such as hydroquinone,[5] carbohydrates and alcohols[8], and oxalic acid.[19] In addition to the applications highlighted above, CoO(OH) is an excellent tool for health-related sensors. For example, it has the potential for use in the control of diabetes, where there is a need for the development of reliable glucose-monitoring instruments. The glucose monitoring is standard in clinical laboratories for biochemical diagnostics,[2,20] in the food processing and beverage industries,[2] requiring accurate, sensitive and rapid methods, easy operation and low cost.[5] The most widely employed methods used currently for glucose detection are those involving the enzyme glucose oxidase (GO_x).[20] However, these methods are expensive,[21] and present a range of problems such as instability, inactivity, and thermal and chemical deformation/denaturing.[2]

We report the effect of precursor salts (acetate and nitrate) in the preparation of the colloidal cobalt oxyhydroxides method to evaluate the influence of these salts in the chemical composition, morphology, and electrochemical activity. Cyclic voltammetry measurements were performed to evaluate the use of colloids as an electrode modifier for use as a non-enzymatic sensor for measuring glucose.

2. Experimental

2.1. Materials and Methods

The following reagents were utilized during our study: cobalt(II) acetate tetrahydrate ($Co(CH_3COO)_2{\cdot}4H_2O$, CoOAc, Synth, 99 %); cobalt(II) nitrate hexahydrate ($Co(NO_3)_2{\cdot}6H_2O$, CoNit, Vetec, 98 %); glycerine ($C_3H_5(OH)_3$, gly, Vetec, 99.5 %); n-butanol (C_4H_9OH, n-BuOH, Vetec, 99.4 %); sodium hydroxide (NaOH, Vetec, 97 %); and glucose ($C_6H_{12}O_6$, Glu, Biotec, 99 %). A stock solution of the glucose analyte (5 × 10^{-5} mol L^{-1}) was prepared immediately before use in ultrapure water.

2.2. Synthesis of Colloidal Cobalt Oxyhydroxides – CoO(OH)

The precursor of interest, CoOAc (3.9 mmol, 0.9681 g) or CoNit

* To whom correspondence should be addressed. E-mail: anaissi@unicentro.br

ISSN 0379-4350 Online / ©2017 South African Chemical Institute / http://saci.co.za/journal
DOI: http://dx.doi.org/10.17159/0379-4350/2017/v70a20

(2.7 mmol, 0.7802 g) was dissolved in glycerine (25 mL) at 50 °C under constant shaking for 90 min. The glycerine promotes the homogeneity of the sample, ensuring chemical stability and long lifetime at cobalt colloidal gelatinous appearance remains unchanged for a period longer than 12 months.[22] A solution of NaOH (n-BuOH, 50 mL, 0.966 M for CoOAc and 0.771 M for CoNit) was added to the cobalt solution, respectively. The mixture was then stirred for 6 h to ensure complete mixing, after which time the mixture was allowed to rest to permit separation of the colloid from the solvent by syneresis. Finally, the samples were washed successive times (at least 5 times) with ultrapure water until constant pH (~10). The conditions resulted in molar proportions: 1.0 Co^{2+}/2.5 OH^- for acetate and 1.0 Co^{2+}/2.0 OH^- for nitrate, and were named colloidal Co_Acetate and Co_Nitrate, respectively. The cobalt colloids were lyophilized, and their precursor salts were pulverized to be characterized for comparison.

2.2.1. *Characterization*

Samples were analyzed by Fourier transform infrared spectroscopy (FTIR) in transmittance mode at 400–4000 cm^{-1} (Nicolet IR 200 spectrophotometer, KBr pellet containing 1 mg sample/100 mg KBr). Simultaneous thermal analysis (TG-DTA) was performed under a nitrogen atmosphere (200 mL min^{-1}) from 30–1000 °C, a heating rate of 10 °C min^{-1}, using alumina as a reference (Seiko TG-DTA/6300). Scanning electron microscopy and energy-dispersive spectroscopy (SEM-EDS) measurements were carried out on a Hitachi TM 3000 microscope, 15 kV electron beam power. The samples were dried at room temperature in aluminum sample holder without metallic coating with gold. UV-Visible (UV-Vis) measurements were performed on an Ocean Optics USB2000 spectrophotometer, equipped with a tungsten-halogen lamp and silicon and germanium detectors, in the diffuse reflectance mode. Cyclic voltammetry (CV) measurements were performed on a Metrohm AUTOLAB potentiostat running Nova 1.8 software, coupled to an electrochemical cell in a conventional three-electrode arrangement: a platinum disc working electrode (1.6 mm diameter), platinum wire counter-electrode, and Ag|AgCl (KCl, 3.0 M) reference electrode. A solution of NaOH (0.5 M) was used as a supporting electrolyte, and gaseous nitrogen was used to purge the solution. All measurements were performed in duplicate. The working electrode (Pt) was modified with an aliquot (1.0 μL) of each colloid (Co.Acetate or Co.Nitrate), deposited by drop on the electrode area, and dried at 25–30 °C to form a thin film.

3. Results and Discussion

To gain a better understanding of the properties of colloidal cobalt oxyhydroxides prepared, they were characterized along with the used precursors. The synthesis of cobalt oxyhydroxides can be problematic, as the resulting compounds display a meta-stable phase that is difficult to isolate on the nanometric scale by conventional methods.[13] The isolation of CoO(OH) requires the stabilization of the Co(III) ion under alkaline conditions, to avoid either the formation of Co_3O_4, a common by-product of the reaction, or the precipitation of cobalt hydroxide.[13] CoO(OH) is therefore composed mainly of trivalent cobalt, although its non-stoichiometric phases often contain a mixture of both Co^{2+} and Co^{3+}.[23]

3.1. Thermal Behaviour (TGA-DTA)

The thermal decomposition curves (Fig. 1) obtained for the precursors (CoOAc and CoNit) and the corresponding cobalt oxyhydroxides (Co.Acetate and Co.Nitrate) enable correlation of the mass loss events with temperature and the assignment of either endothermic or exothermic processes. Three mass loss events were related to the decomposition of the acetate precursor. Firstly, the loss of hydration water takes place, followed by the release of acetic acid,[24] and release of CO_2 (Fig. 1A) is observed. For the nitrate precursor (Fig. 1B), a sequence of events of mass variation about the gradual formation of distinct hydrates takes place, followed by the decomposition of nitrate ions, yielding Co_3O_4 and CoO.[25]

Total weight losses of 69.9 % and 79.3 % recorded in the Co. Acetate and Co.Nitrate colloids, respectively (Fig. 1C,D). Both cobalt oxyhydroxides displayed similar mass loss events, involving the loss of weakly adsorbed or hydration water, decomposition of organic matter (loss of glycerin), and CoO(OH) dihydroxylation.[26] According to the literature, during dehydroxylation at high temperatures, Co_2O_3 and Co_3O_4 are formed under an inert atmosphere (N_2), while metallic cobalt can be generated under a reducing atmosphere (H_2/N_2).[27] Thus, the step corresponding to the final CoO(OH) decomposition step may occur according to Equation 1:

$$2\,CoO(OH) \rightarrow Co_2O_3 + H_2O \quad (1)$$

Table 1 summarizes the processes involving loss of mass (%) and the assignment of events for the cobalt oxyhydroxides and their precursors. It should be noted that the two precursor salts present different decomposition profiles when compared with their corresponding oxyhydroxides.

Nevertheless, the loss of acetate (Fig. 1A) and nitrate (Fig. 1B) ions occurs within the same temperature range as cobalt oxyhydroxide dehydroxylation (Fig. 1C,D). Also, the presence of counterions may be responsible for the differences observed in colloid properties, such the high thermal stability of Co.Nitrate. Loss of these counterions present in the samples may occur close to the third event. Furthermore, a significant percentage of glycerin in the sample composition should be noted. For this reason, and given the nature of cobalt, the resulting colloids are fluorescent, thus making X-ray diffraction plots difficult to obtain due to the presence of wide halos. This characteristic is typical of amorphous materials.

3.2. Scanning Electron Microscopy and Energy-Dispersive Spectroscopy (SEM-EDS)

SEM images (×2500 magnification) show distinct morphologies for both the acetate (CoOAc) and nitrate (CoNit) precursors. The acetate precursor displays features of aggregated particles (Fig. 2A1), while the surface of the nitrate precursor appears more regular and porous (Fig. 2A2). In contrast, the colloid images can be characterized by differences in roughness. While Co.Acetate exhibits a planar surface typical of lamellar materials (Fig. 2A3), Co.Nitrate presents an irregular rough surface with apparent porosity (Fig. 2A4).

Previous literature studies,[23,27] suggest that features such as porosity, large superficial area, and pore volume are essential requirements for the application of these materials as supercapacitors,[23] as they provide a structural basis for high specific capacity.[27] Thus, the size of the film pores, as well as their surface roughness, may improve the redox process, leading to a high packing density of the active material.[27]

Approximate chemical compositions of the Co.Acetate and Co.Nitrate colloids were obtained from the EDS data (Fig. 2B). Considering only cobalt and oxygen atoms, a high degree of purity can be estimated without interfering electroactive components. The percentages of atomic cobalt in the samples were 39.60 % for Co.Acetate, and 46.19 % for Co.Nitrate, corres-

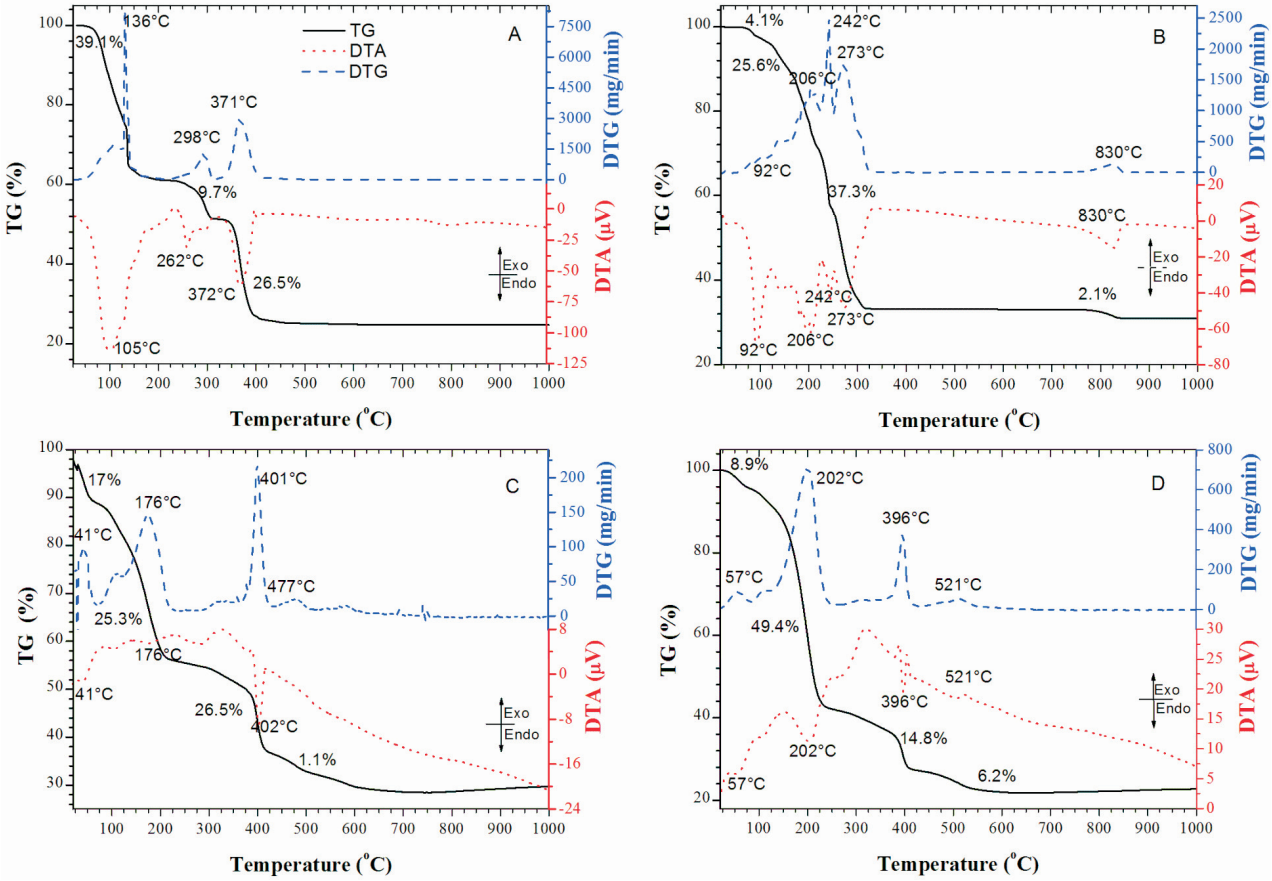

Figure 1 Thermal analysis curves (TGA-DTA) of precursors (**A**) CoOAc and (**B**) CoNit and colloids (**C**) Co.Acetate and (**D**) Co.Nitrate. Conditions: 30–1000 °C, heating rate 10 °C min^{-1}, N_2 atmosphere.

ponding to 1.16 times additional ions exposed on the surface of Co.Nitrate. To estimate the composition of the oxyhydroxides formed quantitatively, these calculations were complemented with TGA-DTA data on mass loss (Fig. 1).

3.3. Fourier Transform Infrared Spectroscopy (FTIR)

Figure 3 shows the FTIR spectra of the cobalt oxyhydroxides, indicating the presence of the OH^- functional group, attributed glycerine (propane-1,2,3-triol). The wide bands observed at 3384–3392 cm^{-1} correspond to the axial deformation of OH^- groups in intermolecular hydrogen bonds,[23] and/or water.[7,24] An additional band was also observed at 1631–1640 cm^{-1}, which can be assigned to the presence of water molecules, thus confirming that both OH^- groups and water molecules are present in the cobalt colloids.[7]

Two bands observed between 2936–2948 and 2881–2875 cm^{-1}

Table 1 Analytical data (TGA-DTA) involving mass loss processes of colloids and their precursors.

Sample	Δm/%	Mass/mg	ΔT*/°C	Assignment	Type of energy
Salt $Co(CH_3COO)_2$	39.1	7.16	30–200	H_2O (hydration)	endo
	9.7	1.77	220–325	H_3COOH	endo
	26.5	4.85	325–500	CO_2	endo
Colloid Co.Acetate	17.0	0.55	30–130	H_2O (adsorbed)	endo
	25.3	0.81	130–280	$C_3H_5(OH)_3$	exo
	26.5	0.85	280–430	OH	endo
	1.1	0.04	440–670	Traces	endo
		Estimated composition:		$CoO(OH)_4 \cdot (gly)_{0.67} \cdot 2.33H_2O$	
Salt $Co(NO_3)_2$	4.1	0.57	30–120	H_2O (hydration)	endo
	25.6	3.58	120–224	Hydrates	endo
	37.3	5.21	225–385	NO_x	endo
	2.1	0.29	706–889	O_2	endo
Colloid Co.Nitrate	8.9	0.69	30–125	H_2O (adsorbed)	endo
	49.4	3.88	125–275	$C_3H_5(OH)_3$	exo
	14.8	1.16	275–450	OH	endo
	6.2	0.48	450–680	Residues	endo
		Estimated composition:		$CoO(OH)_3 \cdot (gly) \cdot H_2O$	

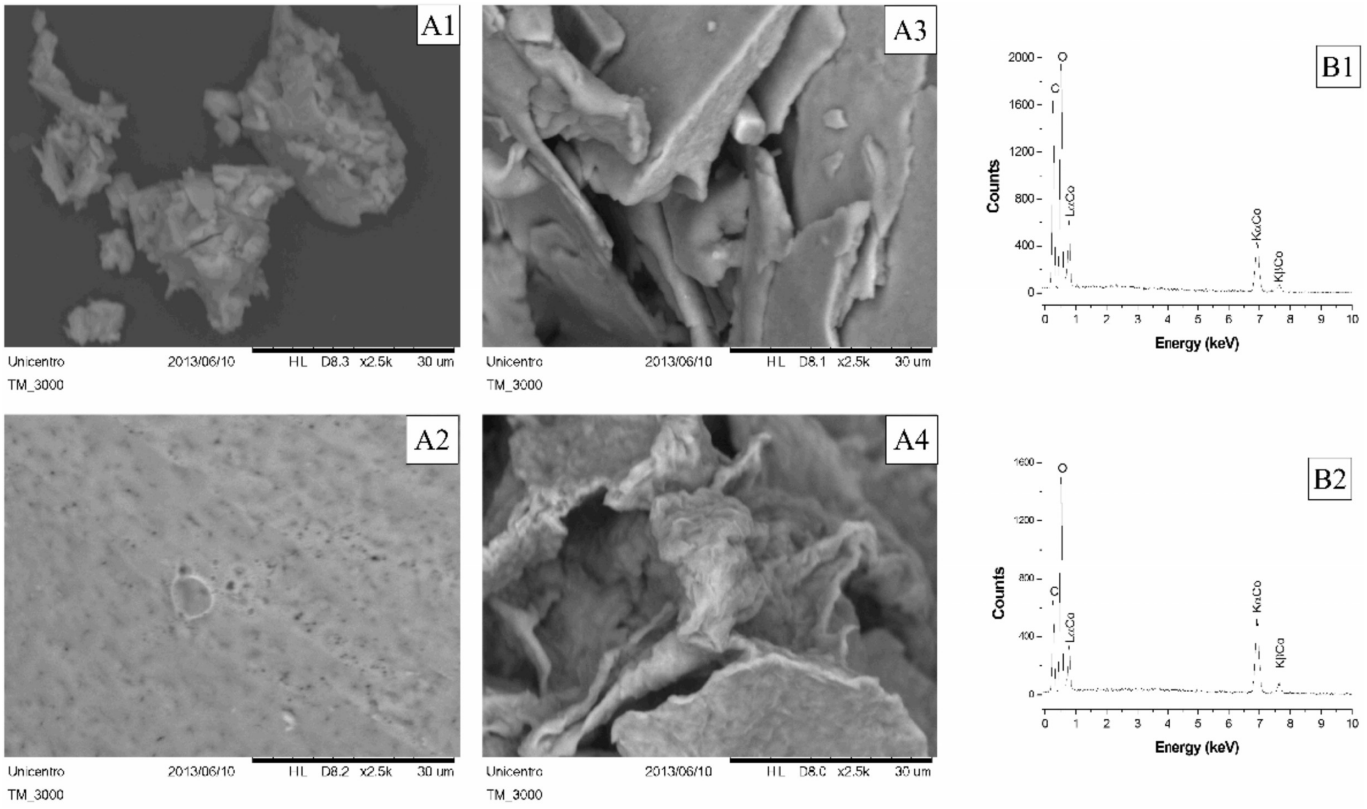

Figure 2 (**A**) SEM images (×2500 magnification) of the precursors: (**A1**) CoOAc and (**A2**) CoNit, and for colloids, (**A3**) Co.Acetate and (**A4**) Co.Nitrate. (**B**) EDS qualitative spectra of the colloids: (**B1**) Co.Acetate and (**B2**) Co.Nitrate.

correlate to the axial deformation of methylene (-CH_2 or =CH_2), while vibrations due to the axial deformation of C-O produce a strong band between 1260 and 1000 cm^{-1}, as can be seen by the sharp band at 1046 cm^{-1}.[23] Finally, bands at 565 and 673 cm^{-1} can be assigned to Co-O vibrations in octahedral and tetrahedral coordination sites, respectively.[26] As expected, some these vibrational modes coincide. However, the presence of a band at 1414 cm^{-1} (Fig. 3A) corresponds to the CH_3COO^- (asymmetric stretching mode) in Co.Acetate, while the intense band at 1384 cm^{-1} corresponds to the presence of the NO_3^- ($\upsilon 3$ vibrational mode) in Co.Nitrate (Fig. 3B).[26] These ions are likely to be intercalated in the colloid structure, while counter-ions are likely derived from the precursor salts.

3.4. UV-Vis Spectroscopy and Band Gap Energy (E_{BG})

With the aim of understanding the differences in colour of the colloids, UV-Vis spectra were collected for both the colloids and the precursors for comparison (Fig. 4). Inorganic salts like cobalt acetate and nitrate, display red-pink colours and so it is expected that multiple absorption bands will be observed in the 350–900 nm region. Both colloids (Co.Acetate and Co.Nitrate) exhibited similar spectral profiles, with the presence of a band between 480 and 520 nm indicating the presence of octahedral Co^{2+} compounds, resulting from $4T_{1g}$ (F) ← $4T_{1g}$ (P) transitions.[28–31] A broadband was also present at 780–790 nm, which may be attributed to low rotation d–d transition of oxyhydroxides for a Co^{3+} species with octahedral coordination, and the $1T_{1g}$(I) ← 1Ag(I) transition,[31] resulting from partial oxidation of the Co^{2+} species, thus leading to a darkening of the samples to give a brown colour.[31]

Cobalt oxides are important p-type semiconductors whose band gap energy (E_{BG}) ranges between 1.48 and 2.19 eV.[29] This energy is a fundamental feature in electrocatalysis, as it corres-

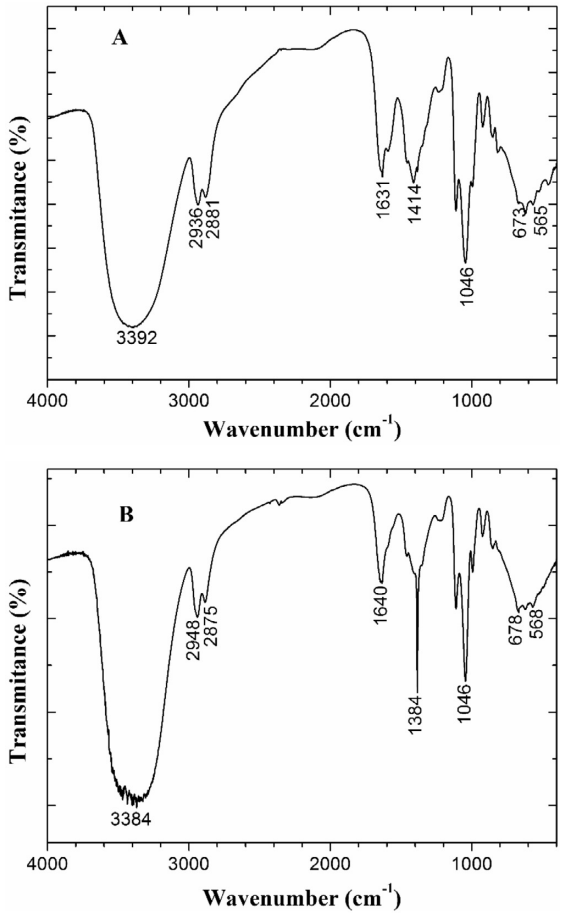

Figure 3 FTIR spectra for both cobalt gels: (**A**) Co.Acetate and (**B**) Co. Nitrate.

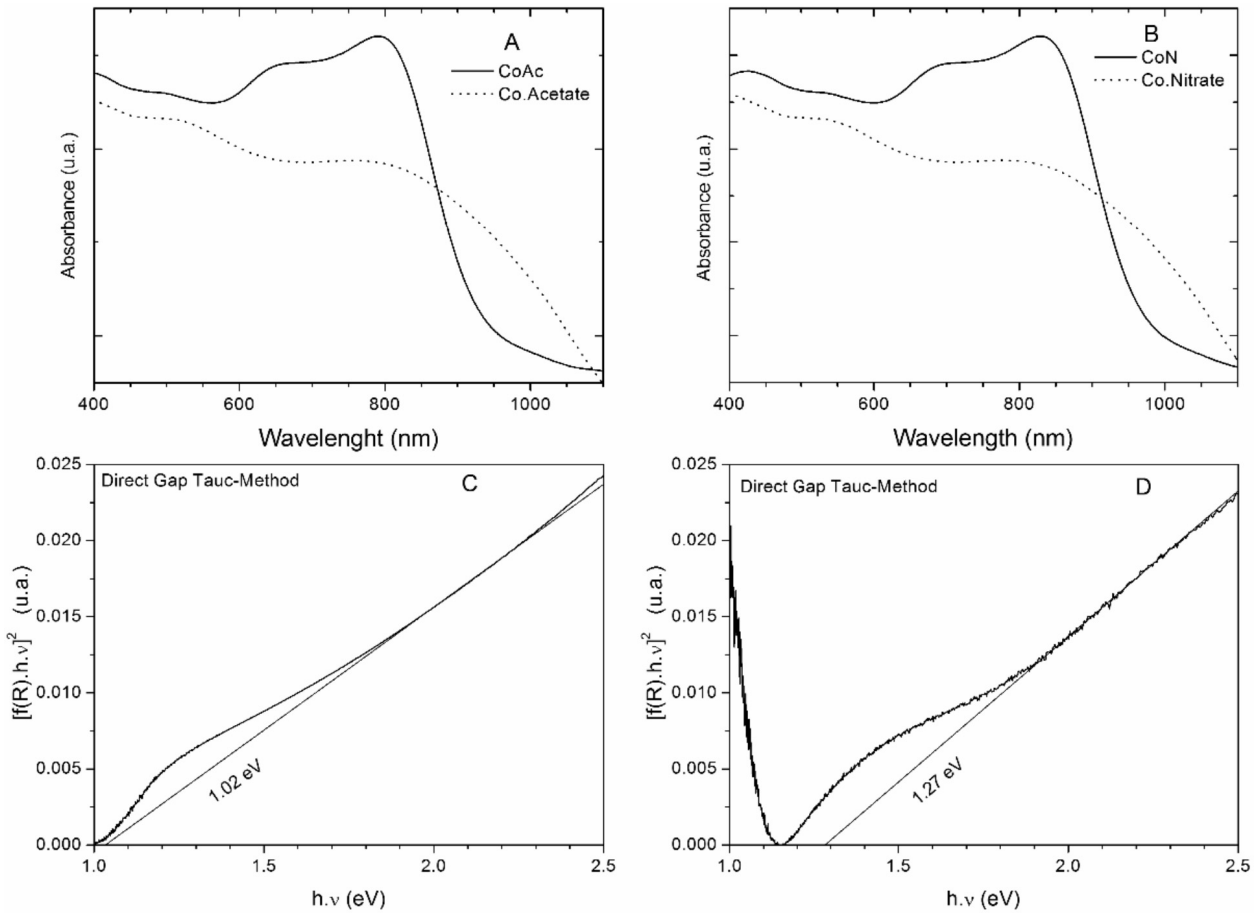

Figure 4 Diffuse reflectance electronic spectra of the colloids and corresponding precursors: (**A**) CoOAc and Co.Acetate, (**B**) CoNit and Co.Nitrate. Energy spectra for band gap assessment using the Tauc method: (**C**) Co.Acetate and (**D**) Co.Nitrate.

ponds to the energy required for electron transition between the valence and conduction bands. Figs. 3C and 3D show the UV-Vis spectra the following conversion into energy spectra, relating the dependence of the function of the sample diffuse reflection ($[f(R)h.\nu]^2$) with radiation energy ($h\nu$). Thus, the band gap energy can be readily determined from a linear regression of the data. Values of 1.02 eV and 1.27 eV were obtained for Co.Acetate and Co.Nitrate, respectively. These values are lower than those reported for cobalt oxides.[32] The E_{BG} values obtained further suggest that the precursor salt, as well as the counterions in the colloid structure, may interfere with the band gap energy of the resulting solid. It has been reported that changes in the E_{BG} may result mainly from the quantum size effect and the presence of an amorphous phase. It is therefore expected that both an increase in crystal size and a decrease in the amorphous phase lead to reduced band gap.[32]

3.5. Chemically Modified Electrodes with Colloidal Cobalt (CME_CoO(OH))

Electrochemical studies were in agreement with the differences observed for cobalt oxyhydroxides. After chemical modification of the working electrode, the film was activated by successive cycling, promoting the definition of the distinctive peaks of cobalt redox processes. Cyclic voltammograms (CVs) were obtained for CME_Co.Acetate (Fig. 5A) and CME_Co.Nitrate (Fig. 5B), with cycling (100 cycles) promoting film stability.

The CVs for both compounds show similar voltammetric profiles, with the presence of 2 pairs of redox peaks and good film stability for both CMEs, even after 100 cycles.[33] In both cases, significant differences were observed between the shift of the peak potential for the first cycle and that of the 100th cycle, although this was more evident for CME_Co.Nitrate. After the 30th cycle, the peak current (E_{p1}) stabilized, becoming the reference for film activation and stabilization. Both colloids showed a shift to negative potentials in the anodic peak (E_{p1}), and a significant current increase with the number of cycles, as summarized in Table 2.

The CV corresponding to the 30th cycle (stabilization cycle) shows similar profiles for both colloids, with the presence of two pairs of redox peaks typical of cobalt (Co^{III}/Co^{II} and Co^{III}/Co^{IV}, Fig. 5C). Interestingly, oxyhydroxide stabilization studies performed by Fan *et al.* (2007) established the 30th cycle as the ideal cycle.[5].

An important factor regarding electrocatalysis is the superficial concentration of the electroactive species (Γ) of cobalt oxyhydroxide on the working electrode. This can be estimated according to Equation 1:[5]:

$$\Gamma = Q/nFA \quad (1)$$

where Γ is the average coating of the surface by the colloid (Co.Acetate or Co.Nitrate) on the surface of the working electrode (mol cm^{-2}), n is the number of electrons transferred in the Co^{3+}/Co^{2+} redox pair (n = 1), F is Faraday's constant (96500 C mol^{-1}), A is the electrode area (2.0×10^{-2} cm^2), and Q is the charge (Coulomb). The charge can be calculated from the area of the Co^{3+} peak in the CV (i.e. the peak with the highest current) and corresponds to the basic charge of the electrode substrate (Table 2).[5]

Although the CMEs show excellent electrochemical responses, with defined redox pairs and relatively stable currents,

Table 2 Electrochemical data obtained from Fig. 4, relating the potentials and anodic peak currents (1st and 100th cycles) with the superficial concentration of the electroactive species for CMEs Co.Acetate and Co.Nitrate.

CME	Cycle	E_{pa}/mV	ΔE_{pa}/mV	I_{pa}/μA	ΔI_{pa}/μA	Q (C)	γ/mol cm^{-2}
Co.Acetate	1°	258	62	185	84	2.405×10^{-4}	1.18×10^{-7}
	100°	196		269			
Co.Nitrate	1°	285	77	136	122	2.565×10^{-4}	1.33×10^{-7}
	100°	208		258			

CME_Co.Nitrate presents a higher superficial concentration of electroactive species (1.33×10^{-7} mol cm^{-2}) then CME_Co.Acetate (1.18×10^{-7} mol cm^{-2}). This higher concentration, along with differences in material composition, contributes to the higher reproducibility and stability of CME_Co.Nitrate, and so this material was chosen for use in the glucose sensor assays.

3.6. Glucose (Glu) Electrooxidation

CME_Co.Nitrate was used as a non-enzymatic Glucose (Glu) electro-oxidation in alkaline medium, using the CV technique with a range of analyte concentrations (~10^{-8} M), to assess the sensitivity and applicability of the colloid. Following the preparation of the CME, 30 cycles were performed to give electrochemical stabilization and subsequent use as a glucose sensor (Fig. 6). A similar procedure was performed using an unmodified electrode (Pt_{naked}), for comparison. A curve of the linear increase in anodic peak current with analyte concentration was inserted (Fig. 6B).

The presence of a redox pair between +0.26 V and +0.16 V of the CV can be attributed to the quasi-reversible Co^{3+}/Co^{2+} redox process. Also, the current increase between +0.53 V and +0.49 V is likely due to the Co^{4+}/Co^{3+} pair, which undergoes a small shift to more negative potentials with the addition of glucose aliquots. Modification of the electrode, therefore, appears to increase the peak current by several orders of magnitude, when compared with the unmodified electrode (Pt_{naked}).

The anodic and cathodic peaks were separated by 80 mV (Co^{3+}/Co^{2+}), corresponding to the conversion between glucose and gluconolactone and *vice versa*, in a quasi-reversible two-electron process that has been widely reported in the literature.[21] The catalytic electrooxidation of glucose is usually assigned to the formation of cobalt hydroxide ($Co(OH)_2$) at the

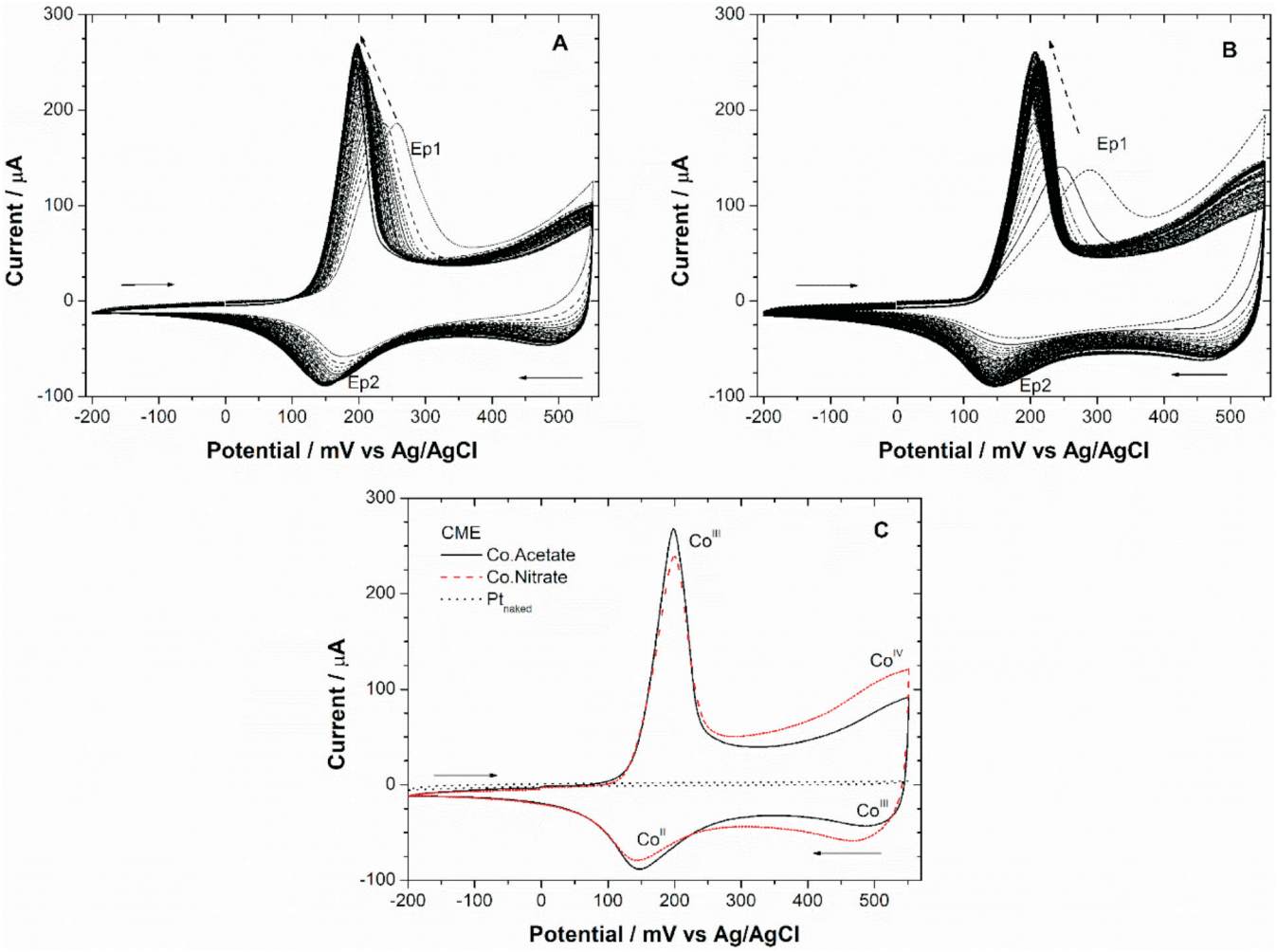

Figure 5 Successive CVs (100 cycles) obtained after electrode pre-activation (10 cycles): (**A**) CME_Co.Acetate, (**B**) CME_Co.Nitrate and (**C**) 30th cycle of the CMEs. NaOH solution (0.5 M), v = 100 mV s^{-1}.

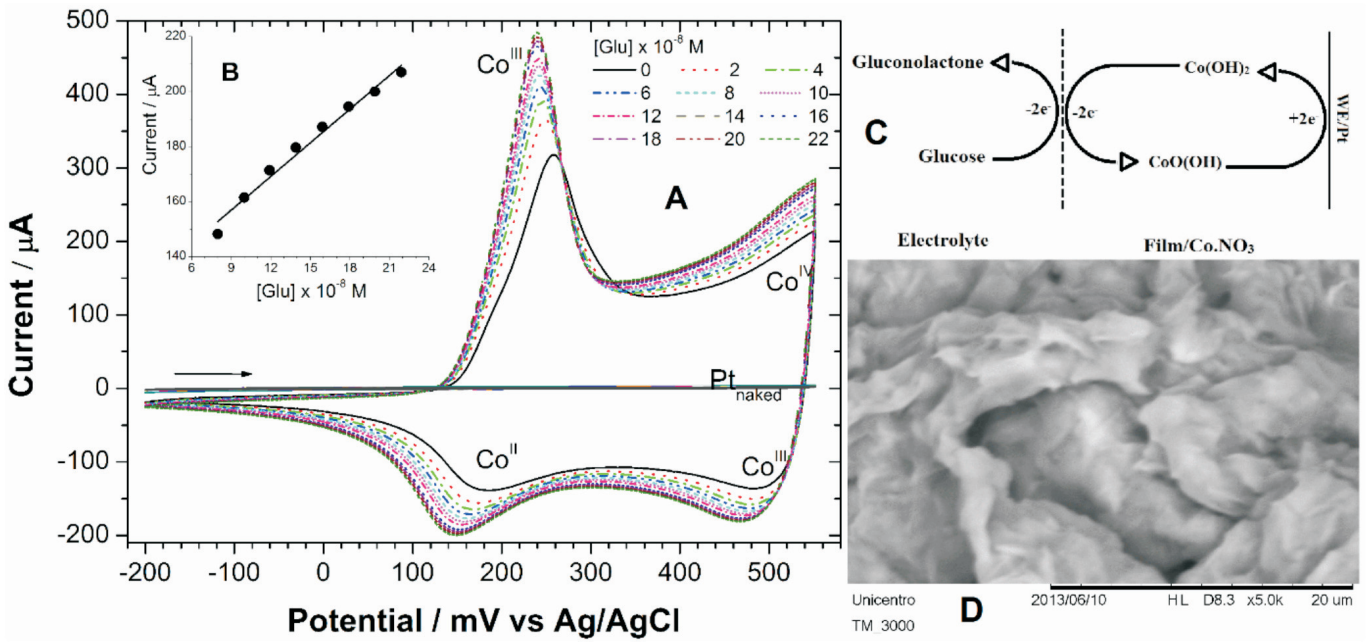

Figure 6 (**A**) CVs of CME_Co.Nitrate and the Pt_{naked} electrode as glucose sensors at different concentrations, in NaOH (0.5 M), v = 100 mV s^{-1}. (**B**) Inset: the anodic peak currents (E_{pa} = 240 mV) and glucose concentration at 2–22 × 10^{-8} M. (**C**) Scheme showing the electro-oxidation involving the redox pair $Co^{III}OH/Co^{II}(OH)_2$. (**D**) SEM image is showing the surface roughness of the CME_Co.Nitrate.

CoO(OH) surface roughness of the CME_Co.Nitrate (Fig. 2A2) and Fig. 2A4). Also, Equation 2 can describe the electrooxidation of glucose, where the oxidation of glucose follows the electrochemical reduction of Co^{3+}/Co^{2+} (Equation 3) to gluconolactone (Equation 4):

$$\text{Glucose} + 2\text{CoO(OH)} \rightarrow \text{Gluconolactone} + 2\text{Co(OH)}_2 \quad (2)$$

$$\text{CoO(OH)} + \text{H}_2\text{O} + 1e^- \rightarrow \text{Co(OH)}_2 + \text{OH}^- \quad (3)$$

$$\text{Glucose} \rightarrow \text{Gluconolactone} + 2e^- \quad (4)$$

Successive additions of the analyte led to a decrease in the concentration of active species at the surface of the electrode (Γ), from 1.33 × 10^{-7} mol cm^{-2} (blank) to 7.78 × 10^{-8} mol cm^{-2} (7.98 × 10^{-8} mol L^{-1} glucose), with a progressive decrease in active sites on the film at the electrode surface, until complete saturation was reached. The parameters (R = 0.980; b = 408, and Sb = 7.98 × 10^{-6}) obtained from the linear curve (Fig. 6) were employed to calculate the limit of detection (LOD = 5.87 × 10^{-8} mol L^{-1}) and the limit of quantification (LOQ = 1.96 × 10^{-7} mol L^{-1}). These data, therefore, demonstrate that the colloid employed in these studies, namely Co.Nitrate, presents high sensitivity when compared with other reports of non-enzymatic glucose sensors, such as CoO(OH) nanosheets, whose detection limit, assessed by differential pulse voltammetry, was 30.9 μM[21].

4. Conclusions

Cobalt oxyhydroxide [CoO(OH)] colloids were prepared from cobalt acetate and cobalt nitrate precursors, respectively. Characterization of a range of analytical techniques revealed some significant differences between the two colloids. The Fourier transform infrared spectra showed vibrational modes that indicate the presence of bands typical of the precursors, namely NO_3^- and CH_3COO^- moieties. Also, the presence of counterions was observed in the thermal analysis curves (TG-DTG-DTA) and was associated with mass loss events. Furthermore, the thermal analysis revealed a higher thermal stability for Co.Nitrate than for Co.Acetate. Examination of the scanning electron microscopy images displays typical distinct features of the colloids and demonstrates that the Co.Nitrate surface exhibits higher roughness than that of Co.Acetate.

The study of the electrochemical behaviour showed that CME_Co.Nitrate shows greater stability and sensitivity for use in voltammetric applications. The assessment of its use as a glucose sensor revealed high reproducibility and sensitivity at low analyte concentrations (~10^{-8} mol L^{-1}), with LOD and LOQ values below those reported in the literature for similar systems. In addition to the above advantageous properties, colloids are relatively easy to manipulate and immobilize, thus leading to a number of potential uses for Co.Nitrate, including as a non-enzymatic glucose sensor for clinical and industrial use.

Acknowledgements

The authors would like to thank the Capes Agency (Nos. 028/2009 and 063/2010), CNPq (Scholarship Researcher No. 305447/2013-0 and Grant No. 447902/2014-8), FINEP (Nos. 01.09.0393.00 and 01.12.0471.00) and Fundação Araucária. A. Stadnik and F.Q. Mariani are appreciative of PhD scholarships granted by DS-CAPES.

References

1 C.-W. Tang, C.-B. Wang and S.-H. Chien, Characterization of cobalt oxides studied by FT-IR, Raman, TPR and TG-MS, *Thermochim. Acta*, 2008, **473**, 68–73.

2 J. Yang, W. Zhang and S. Gunasekaran, A low-potential, H_2O_2-assisted electrodeposition of cobalt oxide/hydroxide nanostructures onto vertically-aligned multi-walled carbon nanotube arrays for glucose sensing, *Electrochim. Acta*, 2011, **56**, 5538–5544.

3 A.D. Jagadale, V.S. Kumbhar and C.D. Lokhande, Supercapacitive activities of potentiodynamically deposited nanoflakes of cobalt oxide (Co_3O_4) thin film electrode, *J. Colloid Interface Sc.*, 2013, **406**, 225–230.

4 J.R. Tobias, J. Wass, I. Panas, J. Ásbjörnsson and E. Ahlberg, Quantum chemical modelling of oxygen reduction on cobalt hydroxide and oxyhydroxide, *J. Electroanal. Chem.*, 2007, **599**, 295–312.

5 L.F. Fan, X.Q. Wu, M.D. Guo and Y.T. Gao, Cobalt hydroxide film deposited on glassy carbon electrode for electrocatalytic oxidation of hydroquinone, *Electrochim. Acta*, 2007, **52**, 3654–3657.

6 J. Yang, H. Liu, W.N. Martens and R.L. Frost, Synthesis and character-

ization of cobalt hydroxide, cobalt oxyhydroxide, and cobalt oxide nanodiscs, *J. Phys. Chem. C*, 2010, **114**, 111–119.

7 A.D. Jagadale, D.P. Dubal and C.D. Lokhande, Electrochemical behavior of potentiodynamically deposited cobalt oxyhydroxide (CoOOH) thin films for supercapacitor application, *Mater. Res. Bull.*, 2012, **47**, 672–676.

8 H. Heli and H. Yadegari, Nanoflakes of the cobaltous oxide, CoO: synthesis and characterization, *Electrochim. Acta,* 2010, **55**, 2139–2148.

9 L. Tao, L. Ying, H. Dengliang and M. Gouhua, Preparation of cobalt nanofibres by means of mild thermal precipitation and thermal decomposition process, *Rare Met. Mater. Eng.,* 2012, **41**, 1527–1530.

10 T. Tsoncheva, A. Gallo, N. Scotti, M. Dimitrov, R. Delaigle, E.M. Gaigneaux, D. Kovacheva, V.D. Santo and N. Ravasio, Optimization of the preparation procedure of cobalt modified silicas as catalysts in methanol decomposition, *Appl. Catal., A*, 2012, **417-418**, 209–219.

11 R.-J. Wu, J.-G. Wu, T.-K. Tsai and C.-T. Yeh, Use of cobalt oxide CoOOH in a carbon monoxide sensor operating at low temperatures, *Sens. Actuators, B*, 2006, **120**, 104–109.

12 T.N. Ramesh and P.V. Kamath, Bi_2O_3 modified cobalt hydroxide as an electrode for alkaline batteries, *Electrochim. Acta*, 2008, **53**, 4721–4726.

13 S.R. Alvarado, Y. Guo, T. Purnima, A. Ruberu, A. Bakac and J. Vela, Photochemical versus thermal synthesis of cobalt oxyhydroxide nanocrystals, *J. Phys. Chem. C*, 2012, **116**, 10382–10389.

14 S. Han, Z. Feng, L. Hu, Y. Li, J. Hao and J. Zhang, Synthesis and electrochemical performance of β-$Co(OH)_2$, *Mater. Chem. Phys.,* 2010, **124**, 17–20.

15 Z. Chang, H. Li, H. Tang, X.Z. Yuan and H. Wang, Synthesis of γ-CoOOH and its effects on the positive electrodes of nickel batteries, *Int. J. Hydrogen Energy,* 2009, **34**, 2435–2439.

16 X. Li, T. Xia and J. Li, Consumption reduction of AB_5 alloy in Ni–MH battery by the use of cobalt oxyhydroxide coated nickel hydroxide, *J. Alloys Compd.,* 2009, **477**, 836–839.

17 S.G. Kandalkar, H.-M. Lee, H. Chae and C.-K. Kim, Structural, morphological, and electrical characteristics of the electrodeposited cobalt oxide electrode for supercapacitor applications, *Mater. Res. Bull.,* 2011, **46**, 48–51.

18 S. Zhuiykov, Carbon monoxide detection at low temperatures by semiconductor sensor with nanostructured Au-doped CoOOH films, *Sens. Actuators, B,* 2008, **129**, 431–441.

19 E.G. Araujo, G.R. Oliveira, E.V. Santos, C.A. Martínez-Huitle, M. Panizza and N.S. Fernandes, Applicability of electroanalysis for monitoring oxalic acid (OA) concentration during its electrochemical oxidation, *J. Electroanal. Chem.,* 2013, **701**, 32–35.

20 Z. Zhang, S. Gu, Y. Ding and J. Jin, A novel nonenzymatic sensor based on $LaNi_{0.6}Co_{0.4}O_3$ modified electrode for hydrogen peroxide and glucose, *Anal. Chim. Acta,* 2012, **745**, 112–117.

21 K.K. Lee, P.Y. Loh, C.H. Sow and W.S. Chin, CoOOH nanosheets on cobalt substrate as a non-enzymatic glucose sensor, *Electrochem. Commun.,* 2012, **20**, 128–132.

22 M. Danczuk, C.V. Nunes Jr., K. Araki and F.J. Anaissi, Influence of alkaline cation on the electrochemical behavior of stabilized alpha-$Ni(OH)_2$, *J. Solid State Electrochem.,* 2014, **18**, 2279–2287.

23 M. Salavati-Niasari, A. Khansari and F. Davar, Synthesis and characterization of cobalt oxide nanoparticles by thermal treatment process, *Inorg. Chim. Acta,* 2009, **362**, 4937–4942.

24 Y. Yang, R. Liu, K. Huang, L. Wang, S. Liu and W. Zeng, Preparation and electrochemical performance of nanosized Co_3O_4 via hydrothermal method, *Trans. Nonferrous Met. Soc. China,* 2007, **17**, 1334–1338.

25 P.M. Crnkovic, C. Koch, I. Ávila, D.A. Mortari, A.M. Cordoba and A.M. Santos, Determination of the activation energies of beef tallow and crude glycerin combustion using thermogravimetry, *Biomass Bioenergy,* 2012, **44**, 8–16.

26 L.F. Cótica, V.F. Freitas, I.A. Santos, M. Barabach, F. J. Anaissi, R.Y. Miyahara and P.W.C. Sarvezuk, Cobalt-modified Brazilian bentonites: preparation, characterisation, and thermal stability, *Appl. Clay Sci.,* 2011, **51**, 187–191.

27 C. Ehrhardt, M. Gjikaj and W. Brockner, Thermal decomposition of cobalt nitrato compounds: preparation of anhydrous cobalt(II)nitrate and its characterisation by infrared and Raman spectra, *Thermochim. Acta,* 2005, **432**, 36–40.

28 L.F. Fan, X.Q. Wu, M.D. Guo and Y.T. Gao, Cobalt hydroxide film deposited on glassy carbon electrode for electrocatalytic oxidation of hydroquinone, *Electrochim. Acta,* 2007, **52**, 3654–3659.

29 J.R.S. Brownson and C. Lévy-Clément, Nanostructured α- and β-cobalt hydroxide thin films, *Electrochim. Acta,* 2009, **54**, 6637–6644.

30 M. Herrero, P. Benito, F.M. Labajos and V. Rives, Stabilization of Co^{2+} in layered double hydroxides (LDHs) by microwave-assisted ageing, *J. Solid State Chem.,* 2007, **180**, 873–884.

31 H. Deng, A.K.L. Teo and Z. Gao, An interference-free glucose biosensor based on a novel low potential redox polymer mediator, *Sens. Actuators, B,* 2014, **191**, 522–528.

32 V. Patil, P. Joshi, M. Chougule and S. Sen, Synthesis and characterization of Co_3O_4 thin film, *Soft Nanosci. Lett.*, 2012, **2**, 1–7.

33 A. Stadnik, E.M. Caldas, A. Galli and F.J. Anaissi, Eletrodo modificado com [CoO(OH)] coloidal aplicado na detecção de ácido oxálico, *Orbital: Electron. J. Chem.,* 2015, **7**, 122–130.